Proceedings of the 30th International Cosmic Ray Conference
Rogelio Caballero, Juan Carlos D'Olivo, Gustavo Medina-Tanco,
Lukas Nellen, Federico A. Sánchez, José F. Valdés-Galicia (eds.)
Universidad Nacional Autónoma de México,
Mexico City, Mexico, 2008
Vol. 1 (SH), pages 429–432

30TH INTERNATIONAL COSMIC RAY CONFERENCE

ICRC'07 Mérida, México

Electron anisotropies in the inner heliosphere

G. S. NKOSI[1], M. S. POTGIETER[1], S. E. S. FERREIRA[1]
[1] *Unit for Space Physics and School of Physics, North-West University, Potchefstroom 2520, South Africa*
fskgsn@nwu.ac.za

Abstract: The COSPIN/KET experiment on board the Ulysses spacecraft has been observing the flux of 3-30 MeV and higher energy electrons in the inner heliosphere (radial distances < 5.2 AU) since its launch in 1990. These observations have indicated the presence of low-energy electrons with a strong anisotropy off the equatorial plane as far as 2.2 AU from Jupiter. This was observed during Ulysses' first encounter with Jupiter in 1992 and again during its descent to low heliospheric latitudes in 2004 when the spacecraft approached Jupiter within 1 AU. A three-dimensional electron modulation model is used to study the modulation of 10 MeV Jovian electron anisotropies in the inner heliosphere. The emphasis is placed on the role that polar perpendicular diffusion plays in establishing a large electron anisotropy in the inner heliosphere.

Introduction

It was discovered by the Pioneer 10 spacecraft [1] and established by the two Voyager spacecraft [2] and the fly-bys of the Ulysses spacecraft [3,4,5] that the Jovian magnetosphere, located at ~ 5.2 AU in the ecliptic plane, is a relatively strong source of electrons with energies of up to ~ 30 MeV. These Jovian electrons propagate along and across the heliospheric magnetic field (HMF) and are observed at Earth and far beyond the Jovian magnetosphere [6]. Since its launch in October 1990, Ulysses has sampled the inner heliosphere in all three dimensions. During this time the Jovian electron intensity has varied significantly with changing heliomagnetic distance to Jupiter and with changing solar activity. In 1992 and 2004, Ulysses had encounters with the Jovian magnetosphere allowing the study of the propagation of electrons originating from this 'point' source in the inner heliosphere. The closest approach to Jupiter was 0.003 AU (6 Jovian radii, R_J) in 1992 and 0.803 AU (1682 R_J) in 2004. Apart from global and temporal effects on electron modulation, such as caused by corotating interaction regions, Jovian electron bursts or jets were also observed during both encounters. These are events with sharp increases and decreases and duration of only a few hours [3]. They were observed as far as 2.2 AU from the planet in 2004. After the 1992 fly-by, jets had also been observed at 0.6 AU from Jupiter, and at north-south displacements of almost 0.5 AU, implying the direct magnetic connection to Jupiter over these distances. In [7,5,8,9] it was noted that these jets seem to come directly along flux tubes from Jupiter with an evident Jovian rotation modulation and having a significant anisotropy, making their identification as the Jovian electrons quite convincing. These extraordinary events are beyond the scope of this paper, but serve as motivation to understand the global electron anisotropy in the inner heliosphere. The modeling described below will give a reference for the interpretation of electron anisotropy observations done by the COSPIN/KET experiment on board Ulysses. Emphasis is on the investigation of the role that polar perpendicular diffusion plays in determining the electron anisotropies in the inner heliosphere. Modeling of the full three-dimensional (3D) anisotropy vector for electrons has not been reported before.

Model and Basic theory

A 3D, steady-state numerical model is used to calculate the three anisotropy components for 10 MeV Jovian electrons in the inner heliosphere. It is based on the numerical solution of Parker's [10] transport equation:

$$\frac{\partial f}{\partial t} = -\left(\mathrm{V} + \langle \mathrm{v_D} \rangle\right)\nabla f + \nabla\left(\boldsymbol{K}_s\ \nabla f\right) + \frac{1}{3}(\nabla\ \mathrm{V})\frac{\partial f}{\partial \ln P} + Q, \quad (1)$$

where $f(\boldsymbol{r}, P, t)$ is the cosmic ray distribution; P is the rigidity, $\boldsymbol{r}$ is the vector position, t is time, and **V** representing the solar wind velocity. The terms on the right hand side represent convection, gradient, and curvature drifts, diffusion and adiabatic energy changes, and the Jovian source function Q. The differential intensity is $j \propto P^2 f$. The diffusion tensor $\boldsymbol{K}_s$ consist of a diffusion coefficient parallel ($K_{\|}$) and perpendicular ($K_{\perp}$) to the average background heliospheric magnetic field (HMF) and is subdivided in two independent coefficients, $K_{\perp\theta}$ and $K_{\perp r}$, which give perpendicular diffusion in the polar and radial direction of the heliosphere respectively. K_A describes gradient and curvature drifts in the large scale HMF. For The general expressions in spherical coordinates for the diffusion coefficients of special interest for this work are:

$$K_{rr} = K_{\|}\cos^2\psi + K_{\perp r}\sin^2\psi,$$
$$K_{\theta\theta} = K_{\perp\theta}, \quad (2)$$
$$K_{\phi\phi} = K_{\perp r}\cos^2\psi + K_{\|}\sin^2\psi, \text{ and}$$
$$K_{\phi r} = \left(K_{\perp r} - K_{\|}\right)\sin\psi\cos\psi = K_{r\phi},$$

where, respectively, Krr, Kθθ, Kϕϕ, Kϕr describe the effective diffusion in the radial direction, in the polar direction, in the azimuthal direction, and in the ϕr-plane; Kϕr can be considered as the 'correction' term which marginally reduces the radial and azimuthal gradients of cosmic rays in Eq. (1). The Parker spiral angle ψ = tan[(r-rs)sinθ/V] is defined as the angle between the radial direction and the average HMF at a certain position, with V the solar wind speed, Ω the angular velocity of the Sun, θ is the polar angle, r is radial distance in AU and rs the Sun's radius. For a typical Parker-type spiral, ψ ~ 450 at Earth, but ψ → 900 beyond 10 AU, and ψ → 00 at the poles.

Concerning perpendicular diffusion, it has become a standard and convenient practice when using modulation models to spatially scale K⊥ as K‖. For K⊥r and K⊥θ it is assumed that

$$K_{\perp r} = 0.02\left(\frac{P}{P_0}\right)^{0.3} K_{\|} \text{ and } K_{\perp\theta} = bK\ F\left(\theta\right) \quad (3)$$

with

$$F\left(\theta\right) = A^+ \pm A^- \tanh\left[\frac{1}{\Delta\theta}\left(\theta_A - 90^0 + \theta_F\right)\right]. \quad (4)$$

Here, P_0 = 1 GV, $a = 0.02(P/P_0)^{0.3}$ and b = 0.015, as required to compute few-MeV electron modulation as shown in [11,12]. According to Eqs. (3) and (4), $K_{\perp\theta}$ is enhanced towards the poles by a factor d with respect to $K_{\|}$ from the value determined by b in the equatorial region. The function $F(\theta)$ in Eq. (4), where $A^{\pm} = (d \pm 1)/2$, $\Delta\theta = 1/8$, $\theta_A = \theta$, and $\theta_F = 35^0$ for $\theta \le 90^0$ while $\theta \ge 90^0$, $\theta_A = 180^0 - \theta$, and $\theta_F = 35^0$.

The anisotropy vector is defined as $\boldsymbol{\xi} = 3\boldsymbol{S}/(4\pi p^2 f)$, with $\boldsymbol{S}$ the streaming vector. In spherical coordinates (r, θ, ϕ), $\boldsymbol{S}$ has three components:

$$\mathbf{S}_r = -4\pi p^2\left[K_{rr}\frac{\partial f}{\partial r} - \frac{K_A\sin\psi}{r}\frac{\partial f}{\partial\theta} + \frac{K_{\phi r}}{r\sin\theta}\frac{\partial f}{\partial\phi} + \frac{V}{3}\frac{\partial f}{\partial\ln p}\right],$$
$$\mathbf{S}_\theta = -4\pi p^2\left[\frac{K_A\sin\psi}{r}\frac{\partial f}{\partial r} + \frac{K_{\perp\theta}}{r}\frac{\partial f}{\partial\theta} + \frac{K_A\cos\psi}{r\sin\theta}\frac{\partial f}{\partial\phi}\right],$$
$$\mathbf{S}_\phi = -4\pi p^2\left[K_{\phi r}\frac{\partial f}{\partial r} - \frac{K_A\cos\psi}{r}\frac{\partial f}{\partial\theta} + \frac{K_{\phi\phi}}{r\sin\theta}\frac{\partial f}{\partial\phi}\right]. \quad (5)$$

From these components, the latitudinal, azimuthal and radial anisotropy components, ξ_r, ξ_θ, ξ_ϕ can be calculated. Following [13] it is assumed that for Jovian and low-energy galactic electrons drifts become negligible, i.e. $K_A \to 0$. This gives significantly reduced and expressions for the anisotropy components:

$$\xi_r = -\frac{3}{v}\left[G_r K_{rr} - G_\phi K_{r\phi} - CV\right],$$
$$\xi_\theta = -\frac{3}{v}\left[G_\theta K_{\perp\theta}\right],$$
$$\xi_\phi = -\frac{3}{v}\left[G_r K_{\phi r} - G_\phi K_{\phi\phi}\right], \quad (6)$$

with G_r, G_θ and G_ϕ the radial, polar and azimuthal gradients, respectively; $C = -1/3(\partial\ln f/\partial\ln P)$ is the

Compton-Getting factor, and v is the particle speed.

It is evident from Eq. (6) that polar perpendicular diffusion plays the dominant role in determining ξ_θ when drifts are neglected. In fact, if ξ_θ and G_θ were to be observed, $K_{\theta\theta}$ could be directly computed for low-energy electrons. On the other hand, for galactic electrons with energies > ~ 100 MeV, drifts cannot be neglected, and ξ_θ becomes significantly more complex, as in Eq. (5).

Results and Discussion

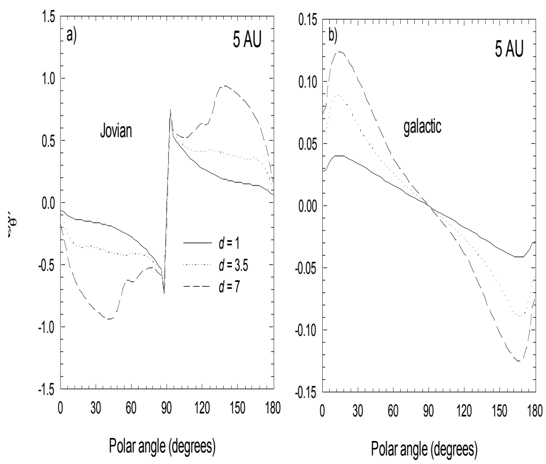

Figure 1: Computed ξ_θ for 10 MeV Jovian (left) and galactic electrons (right) as a function of θ at 5 AU. Three solutions are for d = 1.0 (solid line), d = 3.5 (dotted line) and when d = 7.0 (dashed line), or, alternatively stated, for moderate solar maximum to minimum activity conditions. In this case b = 0.015 and a = 0.006 in Eq. (3).

In the following the modulation effect of different d scenarios on 10 MeV computed Jovian electron anisotropies are shown for b = 0.015 as in Eq. (3). As discussed above, d determines the factor increase in $K_{\perp\theta}$ from the equatorial plane to the heliospheric poles. [14] related the polar angle dependence of V to that for $K_{\perp\theta}$ by using different d-scenarios. They computed the latitude dependence of V in relation to perpendicular diffusion for low-energy electron intensities along the Ulysses trajectory from the end of the first out-of-ecliptic orbit in 1998 to the end of 2003. The d = 1.0 scenario is assumed to correspond to solar maximum conditions, d = 3.5 to intermediate solar activity, and d = 7.0 to solar minimum.

Fig. 1 illustrates the computed latitudinal anisotropy ξ_θ for 10 MeV galactic and Jovian electrons, respectively, in the inner heliosphere as a function of θ. The profiles are shown at a radial distance of 5 AU with the Jovian source at $\theta = 90^0$ and at an azimuthal angle of 0^0. The solid line corresponds to solutions produce when d = 1.0 ($K_{\perp\theta}$ independent of θ), the dotted line to d = 3.5 and the dashed line to d = 7.0. Focusing on the region with $0 \geq \theta \leq 120^0$, the effect of enhancing $K_{\perp\theta}$ is significant for $\theta < 60^0$ and $\theta > 120^0$ and more pronounced for Jovian electrons than for galactic electrons. From Eq. (6) follows that for low-energy electrons ξ_θ is determined by G_θ and $K_{\perp\theta}$.

In Fig. 2 the modulation for the computed magnitude of the total anisotropy vector ξ is shown for the three assumptions for d, along the Ulysses trajectory, with b = 0.015 and a = 0.006 in Eq. (3); in the middle panel separately for Jovian electrons (ξ_{jov}) and galactic electrons (ξ_{gal}); in the lower panel for the combination of 10 MeV Jovian and galactic electrons. The corresponding heliolatitude and radial distance from the Sun of Ulysses are shown in the top panel. For the computed time corresponding to 1991.5, this produces first an increase in the ξ_{tot} ~ 20%, when a good magnetic link to the electron source is encountered. In 1992, a sharp increase up to ~ 38% follows for the first direct encounter with Jupiter, with the closest approach of 0.003 AU. After the 1992 encounter, Ulysses moves south of the planet which in Fig. 2 is shown as the rapid decrease in ξ_{jov} as the spacecraft moves away from the source, but not as sharp as when it approached the planet in the equatorial plane. In 1994, a prominent increase occurs in ξ_{gal}, up to ~3.8%, as the spacecraft moves to the heliospheric poles while the ξ_{jov} clearly subsides. This is followed by a sharp decrease during the first fast latitudinal scan (FLS), with $\xi_{gal} > \xi_{jov}$ up to 1997. The next sharp increase in ξ_{jov} to ~ 20% occurs in 1998, when Ulysses crosses the equatorial plane at 5 AU but with Jupiter on the other side of the Sun. This increase in ξ_{jov} is moderate and similarly shaped as the increase in 1991.5, thus illustrating

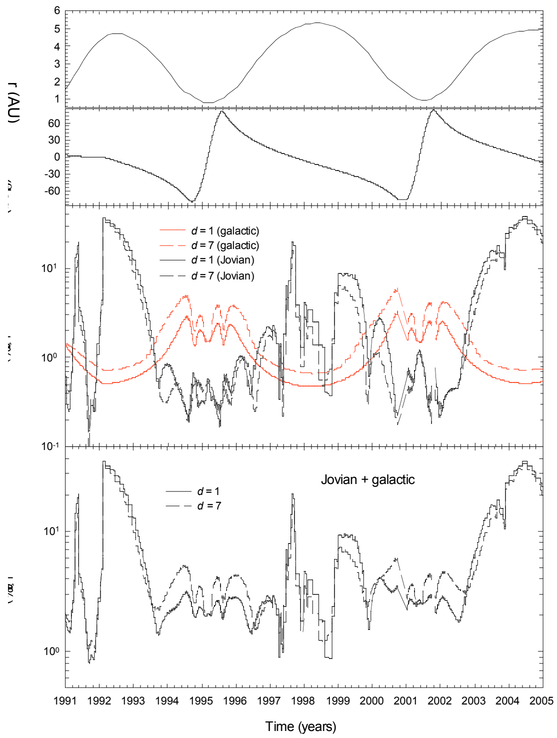

Figure 2: Top panel shows the Ulysses trajectory in radial and heliographic coordinates from 1990 up to 2004. Middle panel shows the computed magnitude of the total anisotropy vector $|\xi|$ as a function of time for 10 MeV Jovian electrons (black lines) and galactic electrons (red lines), for d =1.0 (solid lines) and d = 7.0 (dashed line), with a = 0.006 and b = 0.015 in Eq. (3). In the lower panel, ξ is shown for Jovian and galactic electrons combined.

the effect on ξ when a good magnetic connection is made in the equatorial plane owing to the spiral HMF pattern. In 1999.0 - 1999.8, a sharp increase occurred for ξ_{jov} which had a broad peak with a maximum value of ~ 9% which illustrates again a good magnetic connection to the planet off the equatorial plane. From 2000-2003, $\xi_{gal} > \xi_{jov}$, similar to the previous excursion of Ulysses to high heliolatitudes, followed by the second FLS. This is followed by the distant close encounter in 2004 when Ulysses approaches Jupiter up to 0.804 AU from a northern heliolatitude, thus causing the difference in the shape of the peaks for 1992 and 2004, with the latter significantly wider. The maximum value of ξ_{jov} ~ 38%, similar to 1992, as such a remarkable result. The broader peak in the total anisotropy is indicative of the role of perpendicular diffusion in the latitudinal direction.

Conclusions

In conclusion, it is found using a standard modulation approach, including convection, parallel and perpendicular diffusion but not drifts that the total anisotropy vector for electrons is dominated by the contribution of the Jovian electron anisotropy in the equatorial regions, by as much as a factor of 50 close to the Jovian magnetosphere during solar minimum conditions. Whereas at high heliolatitudes, the galactic electron anisotropy contribution dominates the total anisotropy by a much as a factor of 25. A maximum total anisotropy can be obtained even if only a close encounter of the planet is made but an equatorial approach of the Jovian magnetosphere produces a much sharper anisotropy-time profile than a latitudinal approach. Evidently, the Jovian source of electrons is perfectly suited to study in detail the role of perpendicular diffusion and the predicted enhancement of perpendicular diffusion in the polar direction.

References

[1] J. A. Simpson et al., Science, 183(1974).
[2] R. E. Vogt et al., Science, 206 (1979).
[3] P. Ferrando et al., Planet. Space Sci., 41, 839(1993).
[4] B. Heber et al., Geophys. Res., 107(2002).
[5] H. Kunow et al., Proc. Sol. Wind 11, 2005.
[6] J. H. Eraker, Astrophys. J., 257(1), 862(1982).
[7] B. Heber et al., Planet. Space Sci., 55(2007).
[8] R. B. McKibben, Adv. Space Res., 35(2005).
[9] R. B. McKibben et al., J. Geophys. Res., 110(2005).
[10] E. N. Parker, Planet. Space Sci, 13(1965)
[11] S. E. S. Ferreira et al., J. Geophys. Res., 106 (2001a).
[12] S. E. S. Ferreira et al., J. Geophys. Res., 106 (2001b).
[13] M. S. Potgieter, J. Geophys. Res., 101(1996).
[14] D. M. Moeketsi et al., Adv. Space Res., 35(2005).